



Second harmonic microscopy of monolayer MoS₂

Nardeep Kumar,¹ Sina Najmaei,² Qiannan Cui,¹ Frank Ceballos,¹ Pulickel M. Ajayan,² Jun Lou,² and Hui Zhao^{1,*}

¹*Department of Physics and Astronomy, The University of Kansas, Lawrence, Kansas 66045, USA*

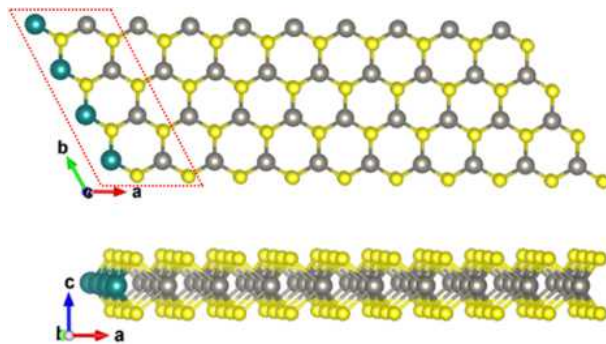
²*Department of Mechanical Engineering and Materials Science, Rice University, Houston, Texas 77005, USA*

(Received 2 March 2013; revised manuscript received 3 April 2013; published 15 April 2013)

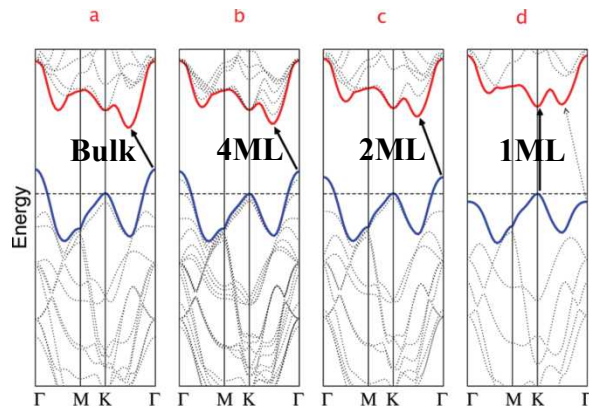
We show that the lack of inversion symmetry in monolayer MoS₂ allows strong optical second harmonic generation. The second harmonic of an 810-nm pulse is generated in a mechanically exfoliated monolayer, with a nonlinear susceptibility on the order of 10^{-7} m/V. The susceptibility reduces by a factor of seven in trilayers, and by about two orders of magnitude in even layers. A proof-of-principle second harmonic microscopy measurement is performed on samples grown by chemical vapor deposition, which illustrates potential applications of this effect in the fast and noninvasive detection of crystalline orientation, thickness uniformity, layer stacking, and single-crystal domain size of atomically thin films of MoS₂ and similar materials.

DOI: [10.1103/PhysRevB.87.161403](https://doi.org/10.1103/PhysRevB.87.161403)

PACS number(s): 42.65.Ky, 78.47.jh, 78.66.Li



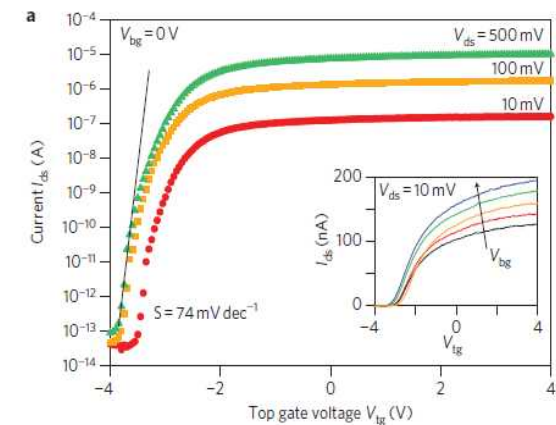
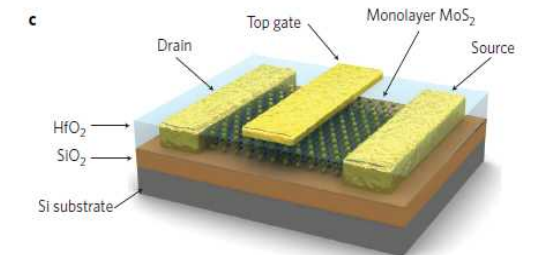
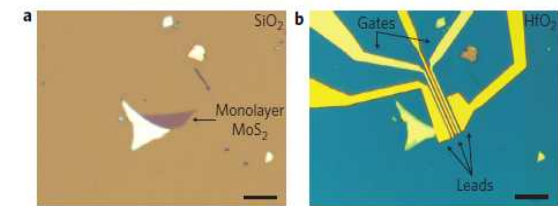
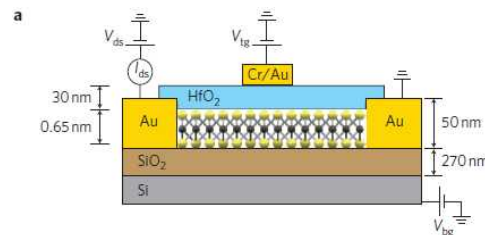
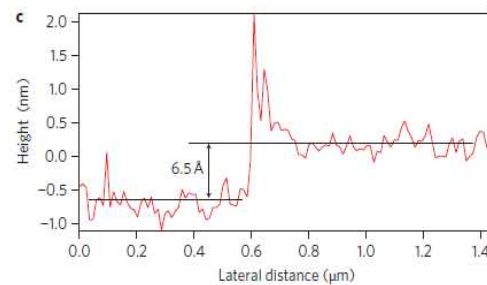
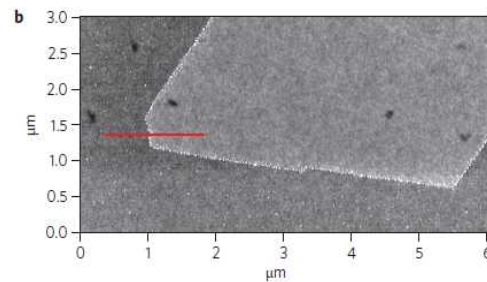
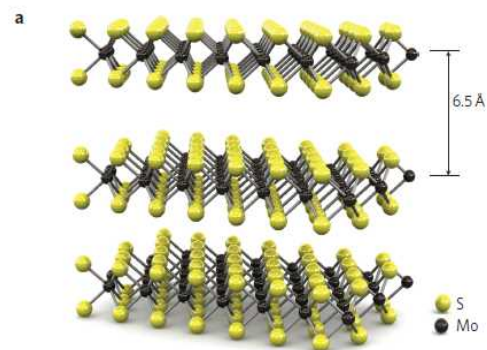
Application of MoS₂ on nanoscale transistor



Splendiani et al. *Nano Lett.* **2010**, *10*, 1271–1275.

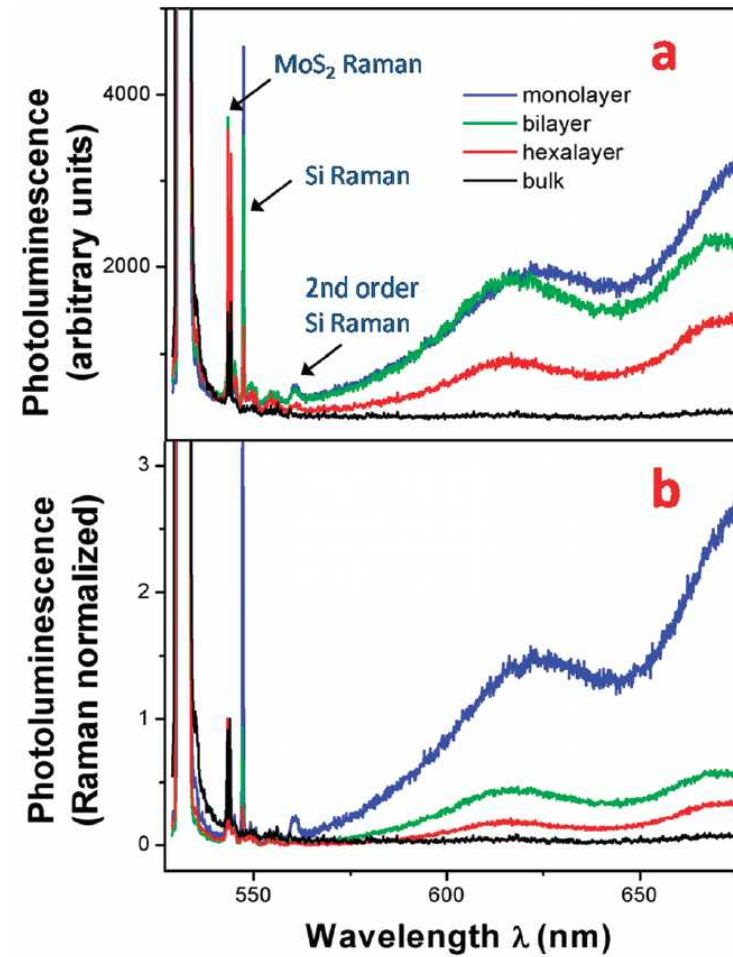
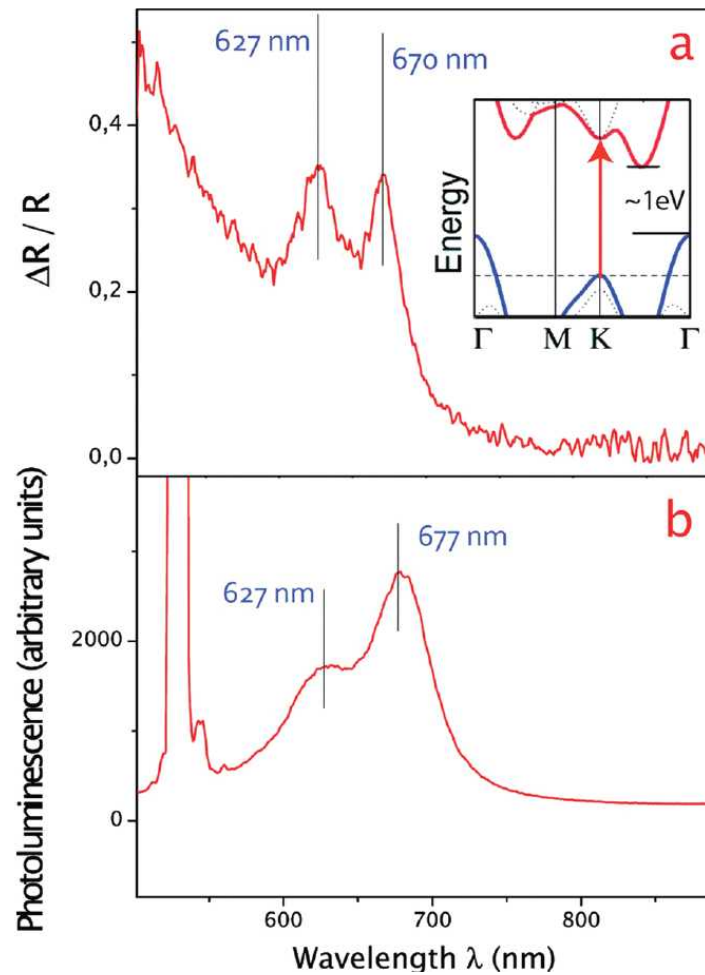
➡ Monolayer MoS₂ has direct band gap (~1.8eV).

➡ Can be applied to FET circuit as channel component.



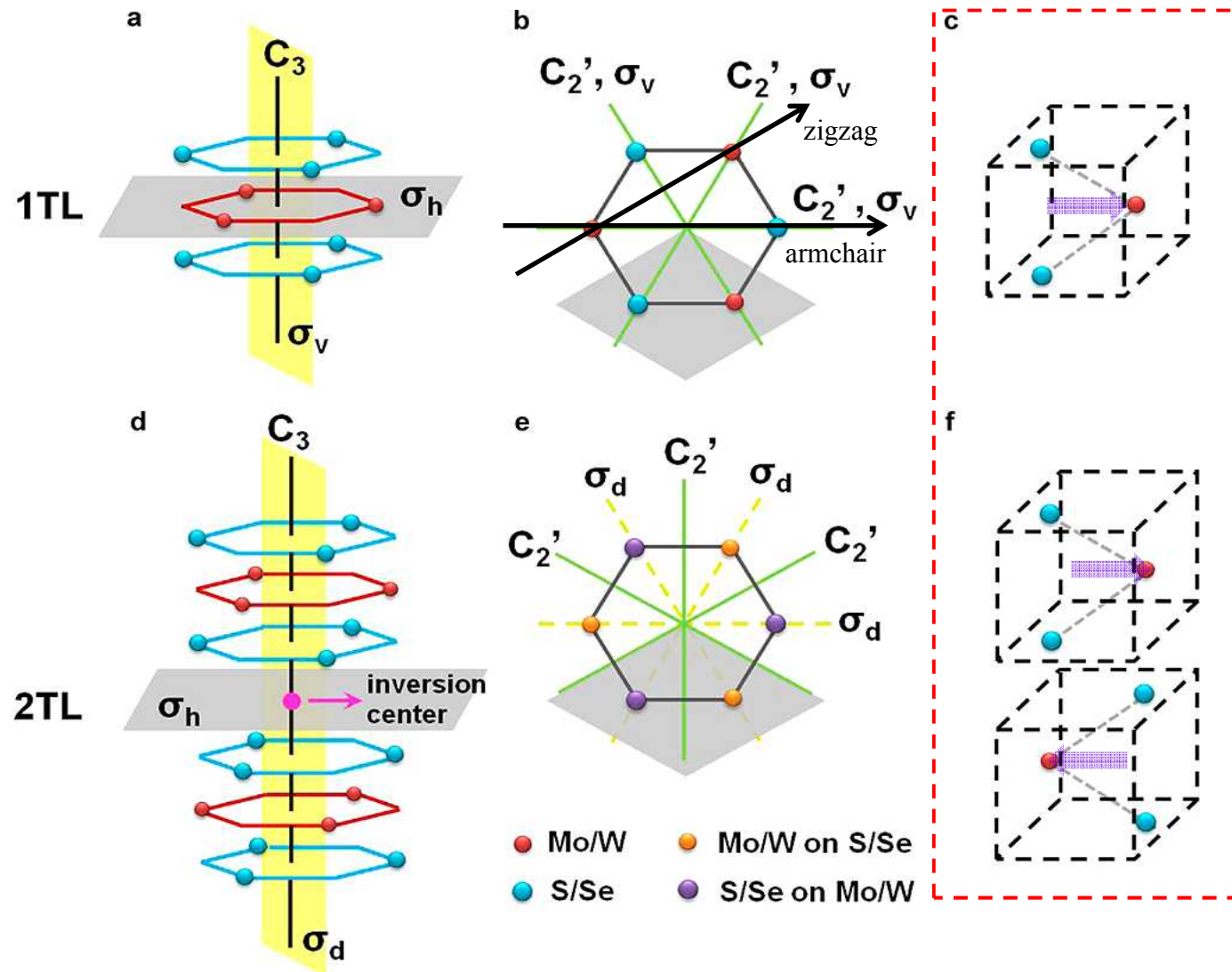
Radisavljevic et al. *Nat. Nanotech.* **2011**, *6*, 147.

Optical properties of MoS₂ thin layer



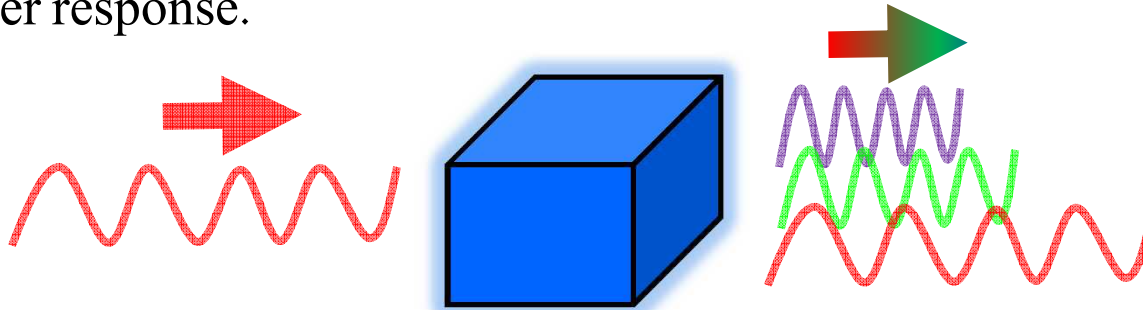
Splendiani et al. *Nano Lett.* **2010**, *10*, 1271–1275.

Structure of MoS₂ : Inversion symmetry broken in odd layer



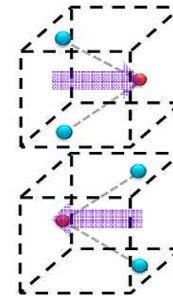
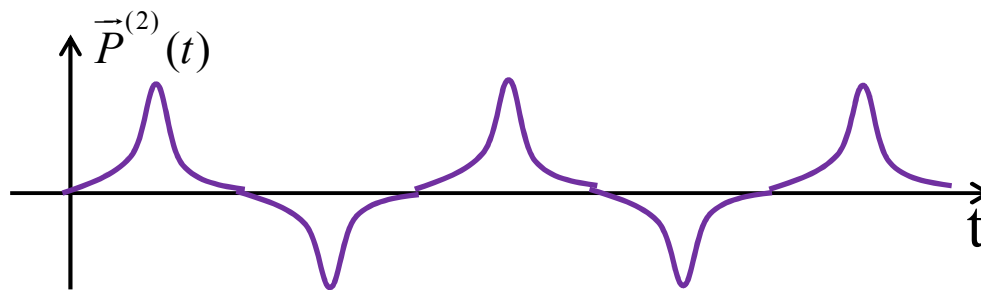
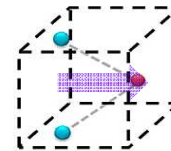
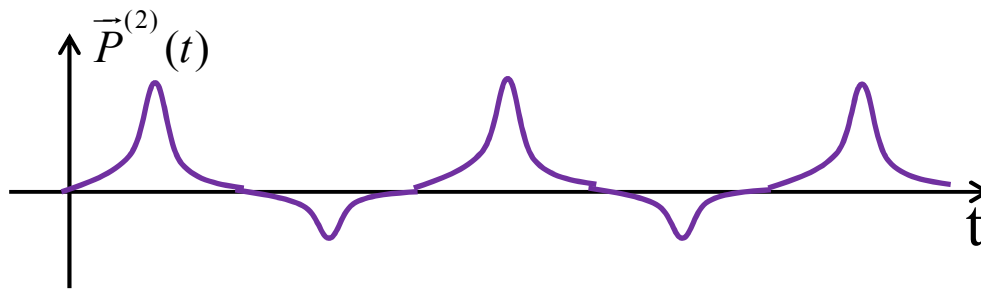
Second harmonic generation occur in noncentrosymmetric media

In the presence of very intense light field (ex-pulsed laser), polarization response has high order response.



Nonlinear responses : Harmonic generation / self-focusing

Linear responses : dispersion / polarization rotation



Setup and sample status

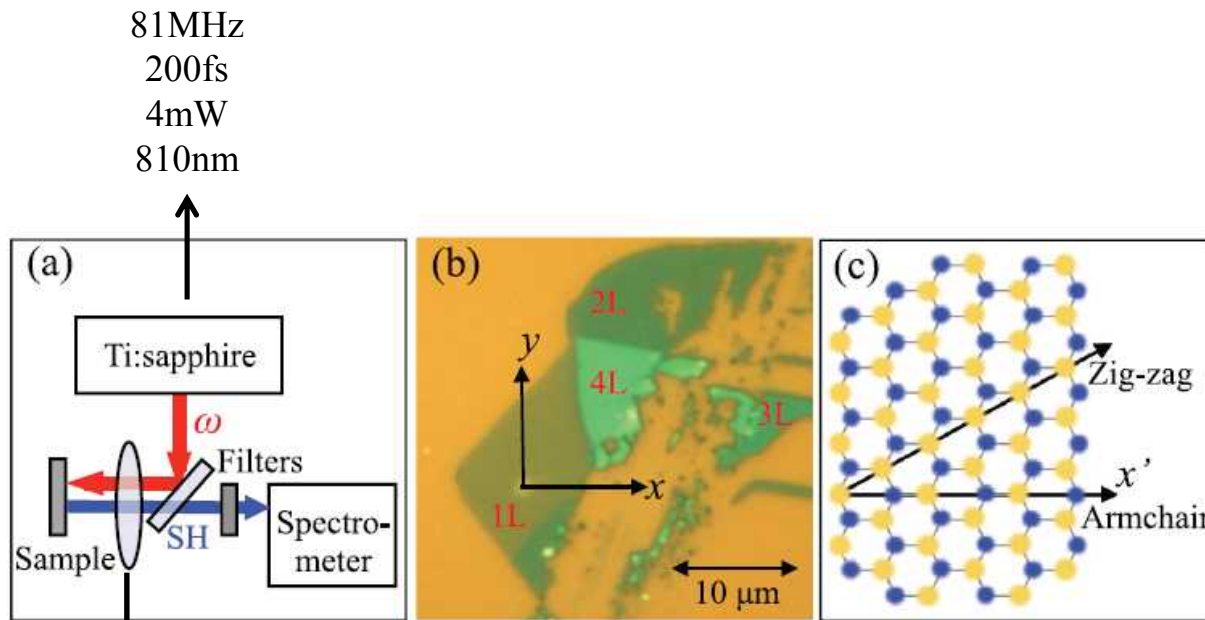


FIG. 1. (Color online) (a) Schematics of the experimental setup. (b) Microscope image of a mechanically exfoliated MoS₂ flake. (c) Lattice structure of monolayer MoS₂.

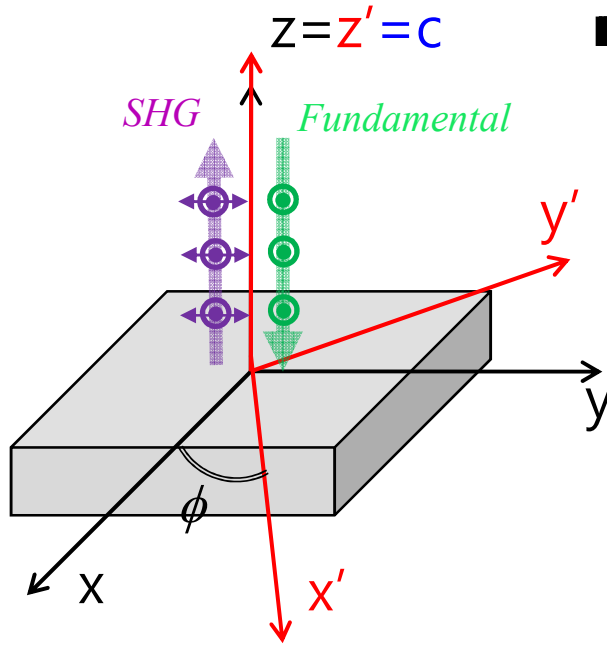
NA=0.15
2r_{fwhm}=2μm
-Peak power at the
sample surface:
~2GW/cm²

For D_{6h} symmetry, second order susceptibility components are,

$$\chi_{y'y'y'}^{(2)} = -\chi_{y'x'x'}^{(2)} = -\chi_{x'x'y'}^{(2)} = -\chi_{x'y'x'}^{(2)}$$

➡ Gives **6-fold symmetry** in SHG intensity with rotation along principal axis (z-axis) – * SHG E-field is **3-fold symmetry**.

Azimuthal angle dependence of SH signal



➔ With respect to the laboratory coordinates (x,y,z), Φ is the rotation angle of sample along z-axis (same as c-axis for MoS₂ monolayer).

$$\chi_{y'y'y'}^{(2)} = -\chi_{y'x'x'}^{(2)} = -\chi_{x'x'y'}^{(2)} = -\chi_{x'y'x'}^{(2)}$$

Effective second order susceptibility :

$$\chi_{eff}^{(2)} = [\hat{e}(\omega_{SHG}) \cdot \vec{L}(\omega_{SHG})] \cdot [\vec{\chi}^{(2)} : [\vec{L}(\omega_{FUN}) \cdot \hat{e}(\omega_{FUN})]^2]$$

$$\chi_{ijk}^{(2)} = (i \cdot i')(j \cdot j')(k \cdot k') \chi_{i'j'k'}^{(2)}$$

(1) In Parallel output, possible component is $\chi_{xxx}^{(2)}$.

$$\begin{aligned} 1) \chi_{xxx}^{(2)} &= \chi_{y'y'y'}^{(2)}(-\sin^3 \phi) + \chi_{y'x'x'}^{(2)}(\cos^2 \phi)(-\sin \phi) + \chi_{x'x'y'}^{(2)}(\cos^2 \phi)(-\sin \phi) + \chi_{x'y'x'}^{(2)}(\cos^2 \phi)(-\sin \phi) \\ &= \chi_{y'y'y'}^{(2)}(-\sin^3 \phi + 3 \sin \phi \cos^2 \phi) = (3 \sin \phi - 4 \sin^3 \phi) = \chi_{y'y'y'}^{(2)} \sin 3\phi \end{aligned}$$

(2) In Perpendicular output, possible component is $\chi_{yxx}^{(2)}$

$$\begin{aligned} 2) \chi_{yxx}^{(2)} &= \chi_{y'y'y'}^{(2)}(\cos \phi)(\sin^2 \phi) + \chi_{y'x'x'}^{(2)}(\cos^3 \phi) + \chi_{x'x'y'}^{(2)}(\sin \phi)(\cos \phi)(-\sin \phi) + \chi_{x'y'x'}^{(2)}(\sin \phi)(-\sin \phi)(\cos \phi) \\ &= \chi_{y'y'y'}^{(2)}(-\cos^3 \phi + 3 \cos \phi \sin^2 \phi) = -\chi_{y'y'y'}^{(2)} \cos 3\phi \end{aligned}$$

Azimuthal angle dependence of SH signal : Result

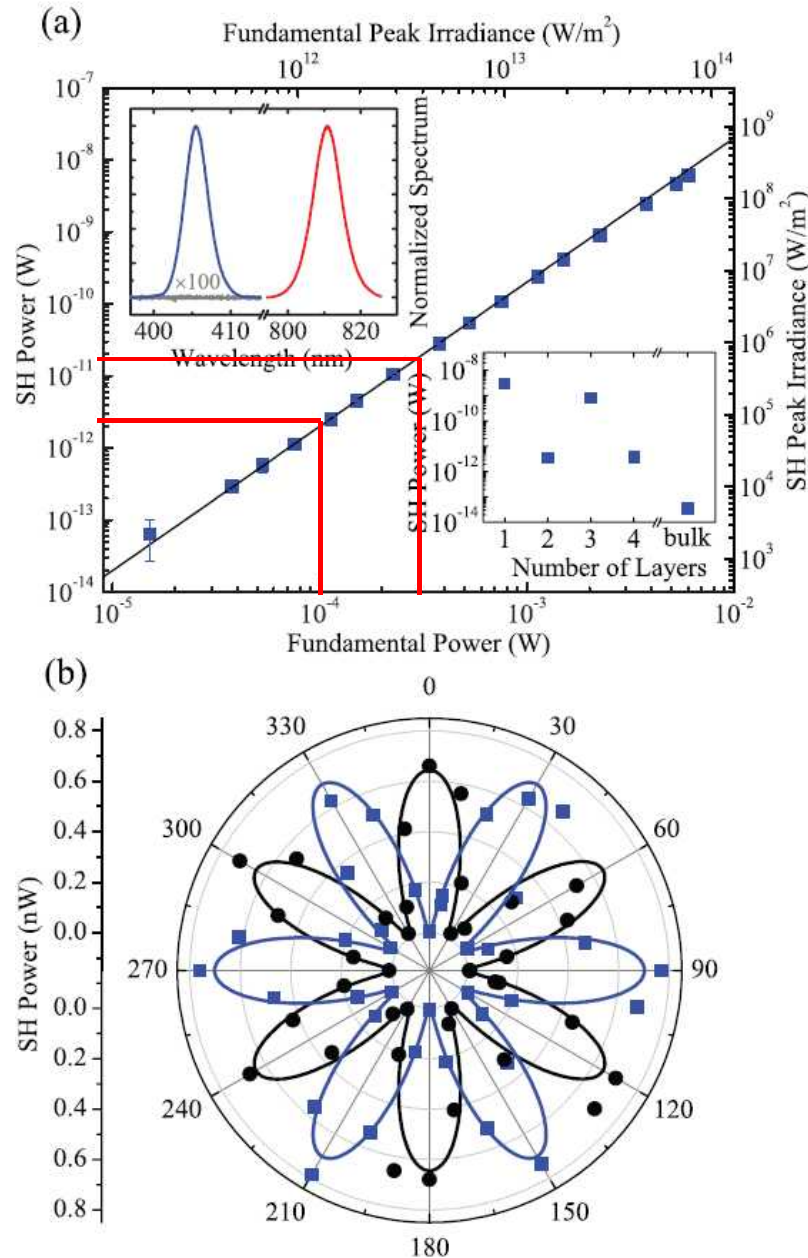


FIG. 2. (Color online) Second harmonic generation from the mechanically exfoliated MoS₂ sample: The upper inset of (a) shows the spectra of the second harmonic from the monolayer MoS₂ (blue) and from the bare substrate (gray, multiplied by a factor of 100), as well as the fundamental beams (red). The lower inset shows the second harmonic power measured from regions with different atomic layers. The main panel of (a) shows the power dependence of second harmonic generation, with the solid line indicating the expected quadratic dependence. (b) The power of parallel (blue squares) and perpendicular (black circles) components of the second harmonic as a function of θ , the angle between the laboratory and the crystalline coordinates. The blue (black) solid line indicates the expected $\sin^2 3\theta$ ($\cos^2 3\theta$) dependence.

$$I_{\text{SHG}} \propto \left| \vec{P}^{(2)}(2\omega) \right|^2 = \left| \vec{\chi}^{(2)} : \vec{E}(\omega) \vec{E}(\omega) \right|^2$$

➡ Quadratic dependence of SHG intensity versus fundamental power.

➡ 6-fold symmetry in SHG intensity vs azimuthal angle indicates that mechanically exfoliated MoS₂ is single crystal.

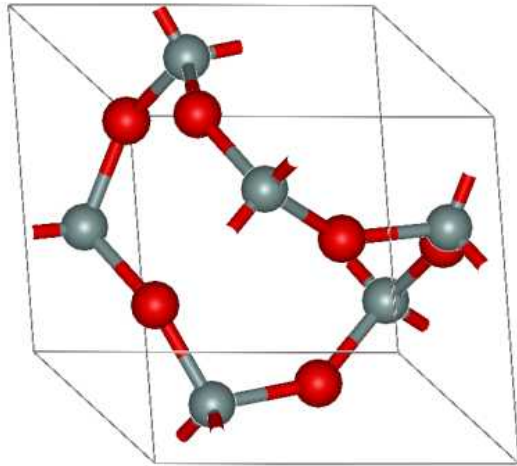
$$\mathcal{E}_x = \frac{1}{4} \frac{i 2\omega}{2n_{2\omega} c} \chi^{(2)} d\mathcal{E}_\omega^2 \sin 3\theta, \quad (1)$$

Determination of $\chi^{(2)}$

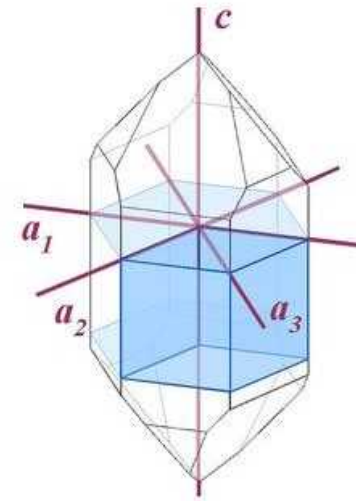
$$\mathcal{E}_x = \frac{1}{4} \frac{i2\omega}{2n_{2\omega}c} \chi^{(2)} d \mathcal{E}_\omega^2 \sin 3\theta, \quad (1)$$

Calculation!!!!

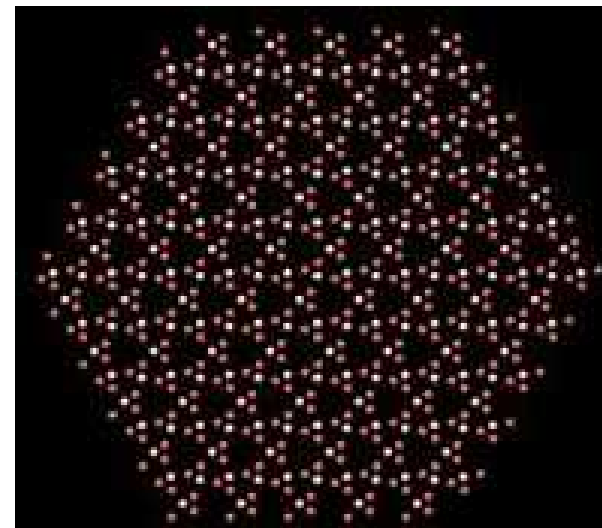
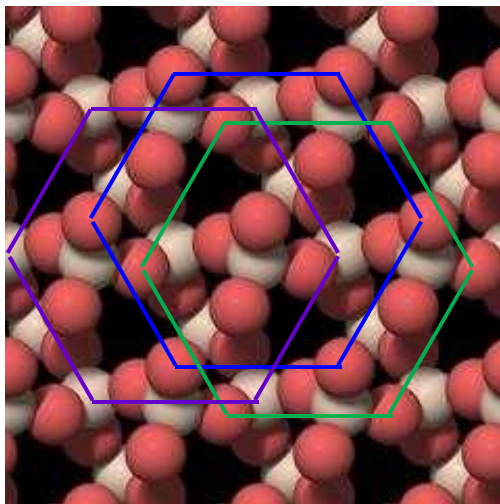
SHG from material having hexagonal lattice : eg) alpha quartz



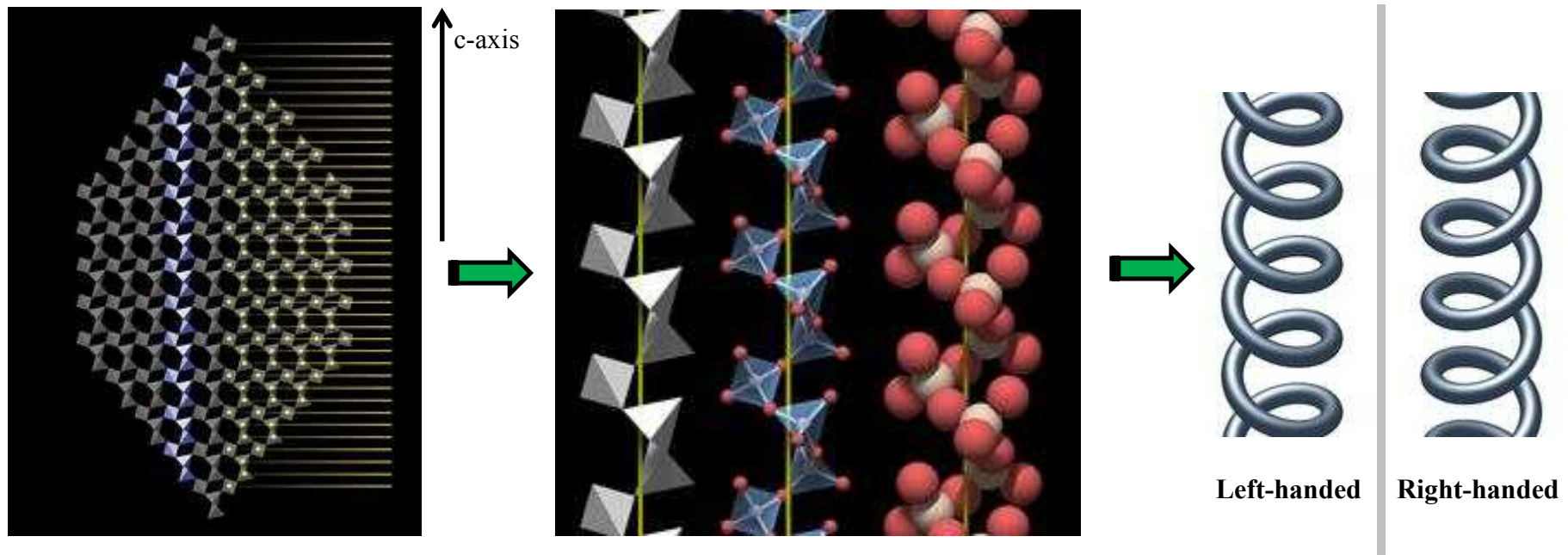
<http://en.wikipedia.org/wiki/Quartz>



http://www.quartzpage.de/gen_struct.html



SHG from material having hexagonal lattice : eg) alpha quartz



Helical structure – no inversion symmetry.

➡ Leading to strong bulk SHG signal.

Allowed second order susceptibility tensor components are,

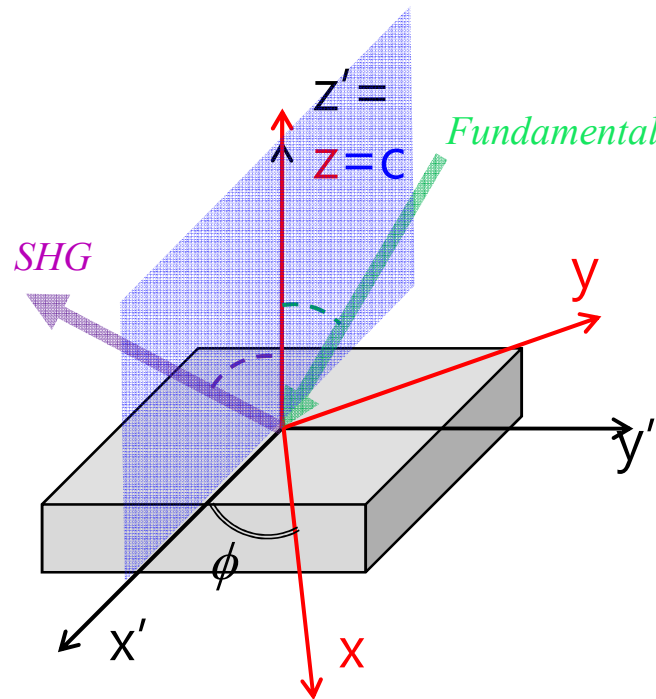
$$\chi_{xxx}^{(2)} = -\chi_{xyy}^{(2)} = -\chi_{yyx}^{(2)} = -\chi_{yxy}^{(2)}$$

$$\chi_{xyz}^{(2)} = -\chi_{yxz}^{(2)}$$

$$\chi_{xzy}^{(2)} = -\chi_{yzx}^{(2)}$$

$$\chi_{zxy}^{(2)} = -\chi_{zyx}^{(2)}$$

SHG from z-cut alpha quartz



➡ With respect to the laboratory coordinates (x', y', z'), ϕ is the rotation angle of quartz along z-axis (same as c-axis for z-cut quartz).

➡ Here, incident plane is x'z' plane. So, unit vector of polarization is \hat{y}' in S-pol, and $\cos \theta \hat{x}' + \sin \theta \hat{z}'$ in P-pol.

Effective second order susceptibility :

$$\chi_{eff}^{(2)} = [\hat{e}(\omega_{SHG}) \cdot \vec{L}(\omega_{SHG})] \cdot [\chi^{(2)} : [\vec{L}(\omega_{FUN}) \cdot \hat{e}(\omega_{FUN})]^2]$$

$$\chi_{ijk}^{(2)} = (i \cdot i')(j \cdot j')(k \cdot k') \chi_{ijk}^{(2)}$$

$$\chi_{xxx}^{(2)} = -\chi_{xyy}^{(2)} = -\chi_{yyx}^{(2)} = -\chi_{yxy}^{(2)}$$

$$\chi_{xyz}^{(2)} = -\chi_{yxz}^{(2)}$$

$$\chi_{xzy}^{(2)} = -\chi_{yzx}^{(2)}$$

$$\chi_{zxy}^{(2)} = -\chi_{zyx}^{(2)}$$

(1) In S-in / P-out , possible components are $\chi_{z'y'y'}^{(2)}$, $\chi_{x'y'y'}^{(2)}$.

$$1) \chi_{z'y'y'}^{(2)} = \chi_{zxy}^{(2)} (\sin \phi)(\cos \phi) + \chi_{zyx}^{(2)} (\cos \phi)(\sin \phi) = 0 \text{ And, all the other calculations including z should be vanished.}$$

$$2) \chi_{x'y'y'}^{(2)} = \chi_{xxx}^{(2)} (\sin^2 \phi)(\cos \phi) + \chi_{xyy}^{(2)} (\cos^3 \phi) - \chi_{yyx}^{(2)} (\sin^2 \phi)(\cos \phi) - \chi_{yxy}^{(2)} (\sin^2 \phi)(\cos \phi)$$

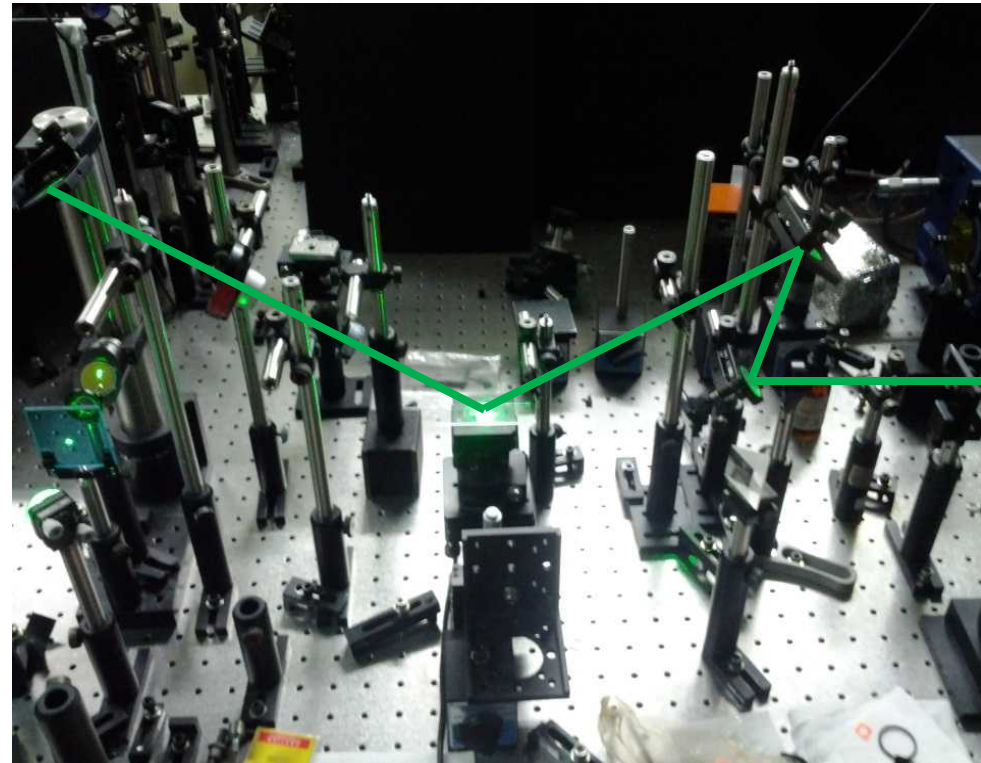
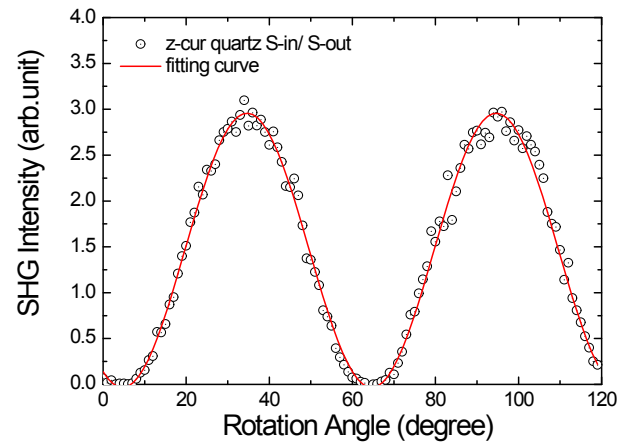
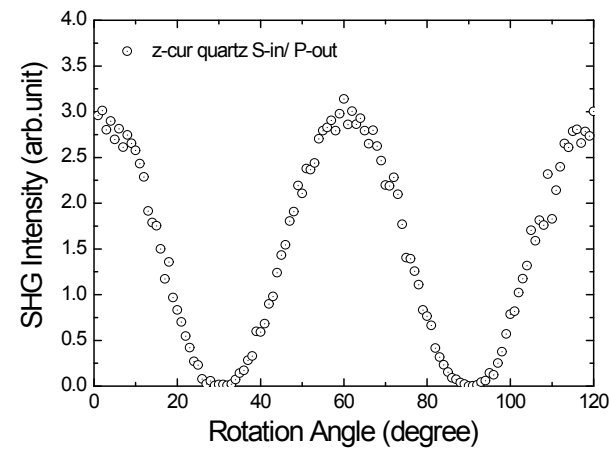
$$= \chi_{xxx}^{(2)} (3 \sin^2 \phi \cos \phi - \cos^3 \phi) = -\chi_{xxx}^{(2)} (\cos 3\phi) \dots \text{ has maxium at } \phi=0^{\circ}, \text{ minimum at } \phi=30^{\circ}$$

SHG from z-cut alpha quartz

(2) In S-in / S-out , possible component is $\chi_{y'y'y'}^{(2)}$

$$\chi_{y'y'y'}^{(2)} = \chi_{xxx}^{(2)}(\sin^3 \phi) + \chi_{xyy}^{(2)}(\sin \phi)(\cos^2 \phi) + \chi_{yyx}^{(2)}(\sin \phi)(\cos^2 \phi) + \chi_{yxy}^{(2)}(\sin \phi)(\cos^2 \phi)$$

$$= \chi_{xxx}^{(2)}(4\sin^3 \phi - 3\sin \phi) = -\chi_{xxx}^{(2)}(\sin 3\phi) \cdots \text{has maximum at } \phi=30^\circ, \text{ minimum at } \phi=0^\circ$$



SHG measurements on CVD MoS₂ film

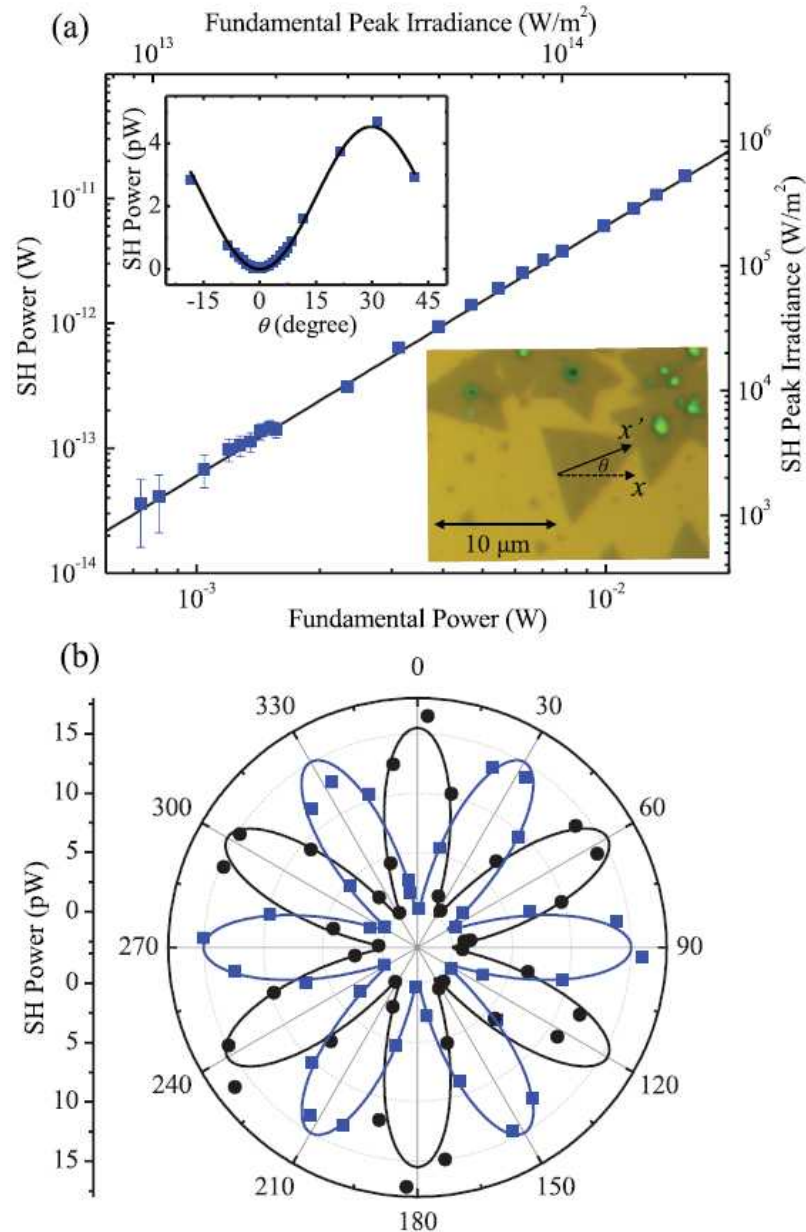


FIG. 3. (Color online) Second harmonic generation from a triangular monolayer MoS₂ flake grown by CVD, as shown in the lower inset of (a). The main panel of (a) shows the power dependence of second harmonic generation. The solid line indicates the expected quadratic dependence. (b) shows angular dependence of the parallel (blue squares) and perpendicular (black circles) components of the second harmonic, along with the expected dependence (solid lines). The upper inset of (a) shows a separate measurement of the parallel component with a finer step size near $\theta = 0^\circ$.

SHG mapping of CVD MoS₂ film

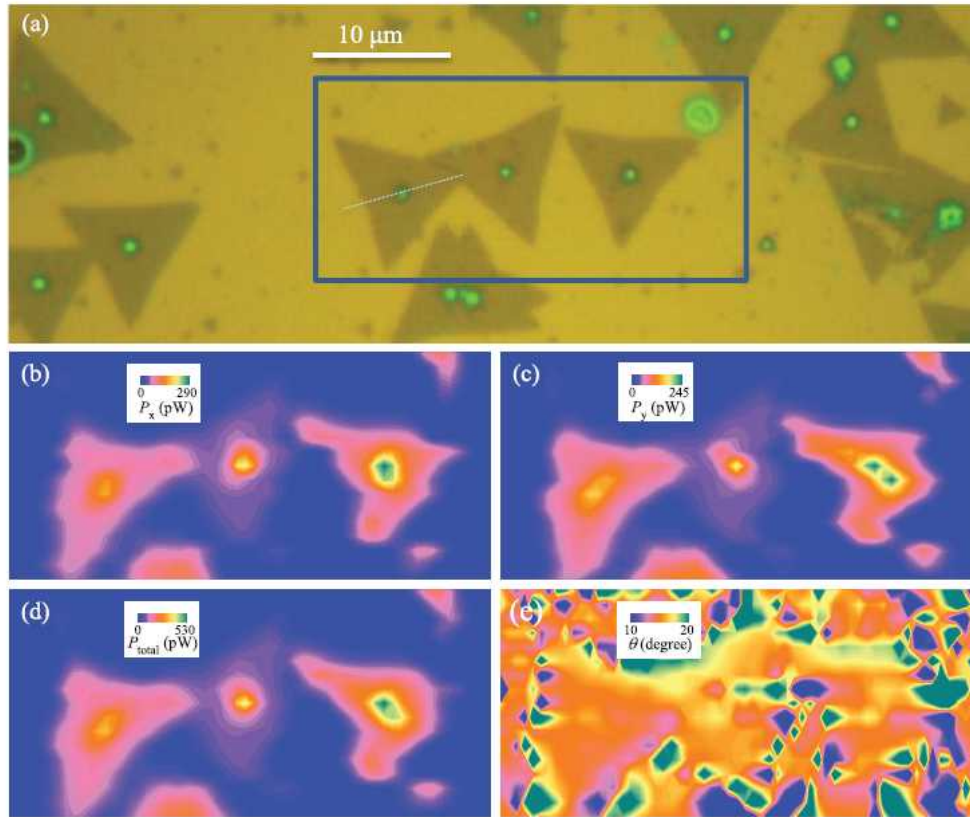


FIG. 4. (Color online) (a) Optical microscopy photograph of a region of a substrate containing flakes grown by CVD. (b) and (c) Maps of P_x and P_y over the region indicated by the box in (a). (d) Map of the total power, $P_x + P_y$. (e) Map of θ calculated from (b) and (c).

Summary

